Eur. Phys. J. A **8**, 131–136 (2000)

THE EUROPEAN PHYSICAL JOURNAL A

Effects of the form factor on exclusive (e, e′p) reactions

K.S. Kim[1,a], Myung Ki Cheoun[1], Il-Tong Cheon[1], and Yeungun Chung[2]

[1] Department of Physics, Yonsei University, Seoul, 120-749, Korea
[2] Department of Physics, Yosu National University, Yosu, 550-250, Korea

Received: 6 December 1999 / Revised version: 21 April 2000
Communicated by Th. Walcher

Abstract. For the exclusive (e, e′p) reaction, we discuss the possibility of observing effects due to swollen nucleons in the nuclear medium, such as ^{40}Ca and ^{208}Pb, by introducing form factors of the nucleon in the nuclear medium. These form factors include effectively the change of nucleon properties in the nuclear medium. This calculation is performed by using a Dirac-Hartree single particle model for a bound state and a relativistic optical model for a continuum state with inclusion of the electron Coulomb distortion. The effect of the form factor, which increases with higher momentum transfer ($q \geq 400\,\mathrm{MeV/c}$) is too small to be discerned from the errors on the available experimental data. But it affects the determination of spectroscopic factors to some extent.

PACS. 25.30.Fj Inelastic electron scattering to continuum – 21.10.Jx Spectroscopic factors

1 Introduction

Exclusive (e, e′p) reactions in the quasielastic region have been one of the most powerful tools to study the nucleon properties in the nucleus, which are believed to differ from those in free space. In the analysis of these (e, e′p) reactions, there have been many attempts even with inclusion of the electron Coulomb distortion[1–5]. These works used the single-particle model [1–3] for obtaining the wave function of a bound state nucleon, while the wave function of an outgoing proton in the final state interacting with the residual nucleus was obtained with a relativistic optical model. The simplest way to analyze the (e, e′p) process is the plane wave impulse approximation (PWIA), in which the final state interactions are not taken into account. In the PWIA the differential cross-section factorizes into two terms. One is the electron-proton cross-section between the incident electron and the bound proton. The other is the spectral function for the probability of finding a proton with given energy and momentum in the target nucleus, which could give us direct information about the nucleons in the nucleus.

In principle, the distortions of the outgoing electron and knockout nucleon, due to interactions with the residual nucleus, could cause a flaw in this factorization. But the recent calculation by Kim *et al.* [2] showed that this factorization is valid even with inclusion of the Coulomb distortions of the electron, *i.e.* in Distorted Wave Born Approximation (DWBA). Moreover their DWBA method, used in this report, is more efficient than other approaches because of fewer parameters. The spectral function obtained this way can be examined through a comparison with experimental data, which is usually presented as the reduced cross-section for the knockout process in electron scattering. Such comparison, however, shows that one needs a scale factor to reproduce the experimental data for a knockout proton near the Fermi energy level [1,2].

The scale factor is commonly interpreted as a spectroscopic factor (SF) for a given state, S_α, which stands for an occupation probability of the nucleon in the given state α. Consequently, the value of the SF is 0 or 1 in the simple single-particle model. But the short-range aspects of nucleon-nucleon interactions in free space give rise to the strong correlation effects between the nucleons in a mean field, for example, a relativistic Hartree [6,7] or Hartree-Fock [8] potential. These correlations lead to a quenching of the occupation probability, so that the SF deviates from its standard value. It should be reminded that the SF extracted this way is an important guideline on the microscopic understanding of the nuclear structure [9].

Therefore many papers were devoted to the extraction of more exact SF values from the theoretical interpretation of the available experimental data. But there are still many ambiguities to be pinned down in those interpretations. For instance, the Gordon ambiguity at electromagnetic vertex function and the Gauge ambiguity at photon propagator could affect this analysis. Our preliminary results [10] show that these ambiguities could affect the final theoretical results by about 10% in the low missing momentum region and by about 20% in the high missing momentum region.

[a] e-mail: kyungsik@phya.yonsei.ac.kr

On the other hand, the nucleon and meson properties are thought to suffer some change in the nuclear medium. Cheon *et al.* [11] had suggested that such change of nucleon properties (masses of nucleon and pion, coupling constant between them) could be expressed in terms of nuclear density by considering the pion's equation of motion in the nucleus. By applying these results to the cloudy bag model of the nucleon, electric and magnetic form factors of the nucleon in the nucleus were obtained. In particular, nucleon charge sizes inside target nuclei, expressed as the root mean square radius, were increased due to such nuclear medium effects. It gives satisfactory explanation of experimental data on coherent electron scattering [11]. We call the increase of the nucleon charge size the effect of swollen nucleons in the nuclear medium. The concept of swollen nucleons has been applied [11–13] to the understanding of the problem of missing strength in the sum rule analysis of the longitudinal response function extracted from inclusive electron scattering. The authors in refs. [11,12] claimed that the missing strength cannot be explained by the RPA theory alone and suggested the modification of the nucleon form factor in the nuclear medium. For ^{40}Ca and ^{56}Fe they showed that the modified proton form factor corresponds to an electromagnetic radius increased by about 20% with respect to the free proton. Recently, Kelly [14] found that the density dependence of nucleon form factors from the quark-meson coupling (QMC) model reduces the polarization ratio at high four momentum transfer, $Q^2 = 0.8\,(\mathrm{GeV/c})^2$, in $(\mathbf{e},\mathrm{e}'\mathbf{p})$ reactions.

In this paper, we try to investigate the swollen effect of the nucleon for $(\mathrm{e},\mathrm{e}'\mathrm{p})$ reactions. One can study the effect by exchanging the form factors of free nucleons into those of nucleons in the nucleus. Since the SF extracted so far is obtained by using those of free nucleons, it would be interesting to reexamine how the swollen nucleon affects theoretical interpretations and the SF. In sect. 2, we briefly discuss the incorporation of the medium effects through the pion's equation of motion with the calculations of the electromagnetic form factors on the cloudy bag model and give the cross-section with the nucleon current. In sect. 3, we insert the modified form factor into the nucleon current used in the analysis of the $(\mathrm{e},\mathrm{e}'\mathrm{p})$ reaction. The bound nucleon wave function is obtained by a relativistic Hartree single-particle model [7], which consists of scalar and vector potentials fitted to the elastic proton scattering data and a relativistic optical model [15] for the outgoing proton is used. The wave functions for incident and final electrons contain the electron Coulomb distortion due to the target nucleus. The SF values are extracted for the two most outer energy orbits in ^{40}Ca and ^{208}Pb by comparing to the NIKHEF data [16,17]. Finally, we give the conclusion in sect. 4.

2 Theoretical formalism

Here we show how to obtain the form factors of the nucleon embedded in a nucleus. Since it is well known that the pion and nucleon masses as well as the pion-nucleon coupling constant are effectively modified in the nuclear medium, we start from the following equation of motion of the pion in nuclear medium characterized by the nuclear density $\alpha(\mathbf{r})$:

$$\big(-\nabla^2 + m_\pi^2\big)\phi_\pi(\mathbf{r}) = \frac{i}{\sqrt{2}}\frac{g_{\pi\mathrm{NN}}}{m_\mathrm{N}}\boldsymbol{\sigma}\cdot\nabla\delta(r) + \nabla\cdot\alpha(\mathbf{r})\nabla\phi_\pi(\mathbf{r}). \tag{1}$$

For a free pion, *i.e.* without the second term on the right-hand side in eq. (1), and for a pion in medium, the solution in momentum space is given by

$$\phi_\pi(\mathbf{q}) = \frac{i}{\sqrt{2}}\frac{g_{\pi\mathrm{NN}}}{m_\mathrm{N}}\frac{\boldsymbol{\sigma}\cdot\mathbf{q}}{\mathbf{q}^2+m_\pi^2}. \tag{2}$$

If $\alpha(\mathbf{r})$ is assumed to be constant, the solution can be found as

$$\phi_\pi(\mathbf{q}) = \frac{i}{\sqrt{2}}\frac{g_{\pi\mathrm{NN}}}{m_\mathrm{N}}\frac{\boldsymbol{\sigma}\cdot\mathbf{q}}{(1+\alpha)\mathbf{q}^2+m_\pi^2}. \tag{3}$$

The second solution can be expressed as in free space:

$$\phi_\pi(\mathbf{q}) = \frac{i}{\sqrt{2}}\frac{g^*_{\pi\mathrm{NN}}}{m^*_\mathrm{N}}\frac{\boldsymbol{\sigma}\cdot\mathbf{q}}{\mathbf{q}^2+m_\pi^{*2}}, \tag{4}$$

where $g^*_{\pi\mathrm{NN}} = g_{\pi\mathrm{NN}}(1+\alpha)^{-3/2}$, $m^*_\mathrm{N} = m_\mathrm{N}(1+\alpha)^{-1/2}$, $m^*_\pi = m_\pi(1+\alpha)^{-1/2}$. The short-range repulsive character of the nuclear force in free space leads to the nuclear short-range correlations inside the nucleus. This effect can be taken into account by introducing the correlation function

$$f(r_{ij}) = 1 - \exp(-\beta r_{ij}^2) \tag{5}$$

into $\alpha(\mathbf{r}) = \alpha f(r_{ij})$. Then the solution of the pion's equation can be found as eq. (4) except

$$g^*_{\pi\mathrm{NN}} \to \tilde{g}^*_{\pi\mathrm{NN}} = g_{\pi\mathrm{NN}}\left(1+\frac{\alpha/3}{1-\alpha/3}\zeta(\beta)\right), \tag{6}$$

where

$$\zeta(\beta) = \frac{1}{2\sqrt{2}}\beta^{-3/2}\int_0^\infty \frac{k^4}{k^4+m_\pi^*}\exp\left(\frac{-k^2}{4\beta}\right)\mathrm{d}k. \tag{7}$$

Similarly we can do the same calculation for $\tilde{f}^*_\pi$. The $\tilde{g}^*$ and $\tilde{f}^*_\pi$ obtained this way are the input data to calculate the electric and magnetic form factors, G_E and G_M, of the nucleon inside the nucleus. The free parameter α above, which was determined to satisfy the experimental data of (e,e') scattering in ref. [18], in principle, can be calculated from the microscopic model based on QCD. In this work we adopt the values from ref. [11], but examine the consequences of some variations by allowing for some model dependence.

The nucleon transition current is given by

$$J_\mu(\mathbf{r}) = e\bar{\psi}_\mathrm{P}(\mathbf{r})\hat{J}_\mu\psi_\mathrm{b}(\mathbf{r}), \tag{8}$$

where $\hat{J}_\mu$ is a nucleon current operator. ψ_P and ψ_b are the wave functions of the knocked-out proton and the bound

state, respectively. For a free nucleon, the operator consists of two parts, the Dirac contribution and the contribution of an anomalous magnetic moment $\mu_{\rm P}$:

$$\hat{J}^{\mu} = F_1\gamma^{\mu} + F_2\frac{i\mu_{\rm P}}{2M_{\rm N}}\sigma^{\mu\nu}q_{\nu}, \tag{9}$$

where the value of $\mu_{\rm P}$ is 1.793. The form factors F_1 and F_2 evaluated at the four momentum transfer squared q_{μ}^2 are related to the electric and magnetic form factor $G_{\rm E}$ and $G_{\rm M}$ by

$$G_{\rm E} = F_1 + \frac{\mu_{\rm P}q_{\mu}^2}{4M^2}F_2, \qquad G_{\rm M} = F_1 + \mu_{\rm P}F_2, \tag{10}$$

which are assumed to take the following standard form:

$$G_{\rm E} = \frac{G_{\rm M}}{(\mu_{\rm P}+1)} = \frac{1}{(1-(q_{\mu}^2/0.71))^2}, \tag{11}$$

where q_{μ} is in units of GeV.

By using these relations the factorized cross-section in plane-wave Born approximation (PWBA) for an unpolarized target is given by

$$\begin{aligned}\frac{{\rm d}^3\sigma}{{\rm d}E_f\,{\rm d}\Omega_f\,{\rm d}\Omega_{\rm P}} = \frac{PE_{\rm P}}{(2\pi)^2}\sigma_{\rm M}\Bigg[&\frac{q_{\mu}^4}{q^4}R_{\rm L} + \left(\tan^2\frac{\theta_{\rm e}}{2} - \frac{q_{\mu}^2}{2q^2}\right)R_{\rm T} \\ &- \frac{q_{\mu}^2}{2q^2}R_{\rm TT}\cos 2\phi_{\rm P} - \frac{q_{\mu}^2}{q^2}\left(\tan^2\frac{\theta_{\rm e}}{2} - \frac{q_{\mu}^2}{q^2}\right)^{1/2}R_{\rm LT}\cos\phi_{\rm P} \\ &- \frac{ihq_{\mu}^2}{q^2}\tan\frac{\theta_{\rm e}}{2}R_{\rm LT'}\sin\phi_{\rm P}\Bigg],\end{aligned} \tag{12}$$

where $\sigma_{\rm M}$ is the Mott cross-section, h is the incident electron helicity, $\theta_{\rm e}$ is the electron scattering angle and $\phi_{\rm P}$ is the azimuthal angle of the outgoing proton. P and $E_{\rm P}$ are the momentum and the total energy of the outgoing proton. The quantities $R_{\rm L}$, etc. are the nuclear structure functions whose detailed forms are given in ref. [2].

In this calculation, we do not change the Dirac form factor F_1 while F_2, which is the Pauli form factor, is changed via anomalous magnetic moments because of the following reasons: i) $F_1(q^2 = 0)$ is constrained by the gauge invariance, *i.e.* Ward-Takahashi identity, so that nucleon charge is preserved in our model. Using this constraint, the parameters in our nucleon model (for example, $f_{\pi qq}$, f_{π}, etc.) are effectively determined. ii) The anomalous magnetic moment $\mu_{\rm P}$ in Pauli form factor, which term is self gauge invariant, has the large contributions from the higher order diagrams mediated by internal pions, whose dynamics are sensitive on the nuclear density in each nucleus. Therefore we allow its variations inside nucleus in our model.

3 Results

In this analysis we calculate the reduced cross-section of the (e, e′p) reaction in a very transparent approximation.

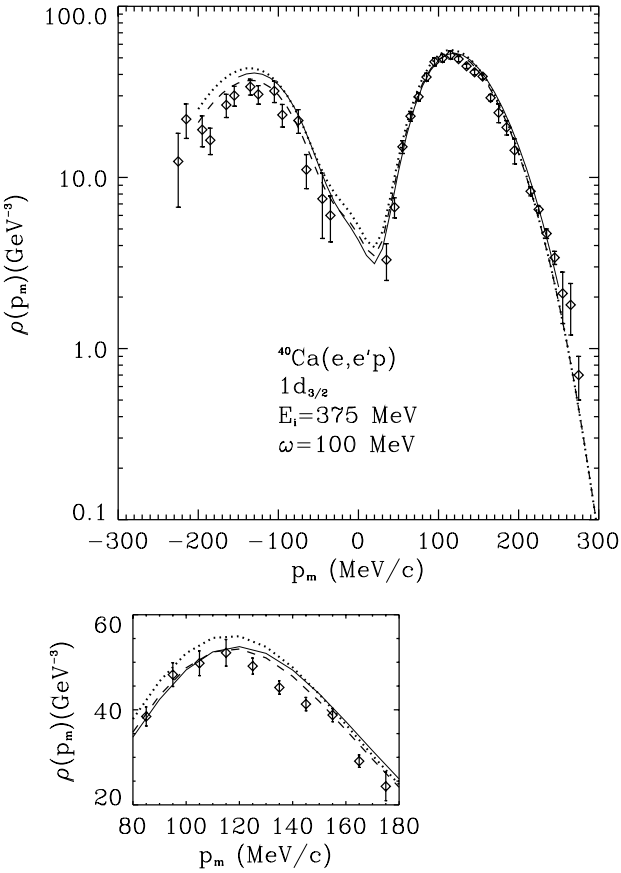

Fig. 1. The reduced cross-sections for proton knocked-out of the $1d_{3/2}$ orbit ^{40}Ca with parallel kinematics. The kinematics are $E_{\rm i} = 375\,{\rm MeV}$, and energy transfer $\omega = 100\,{\rm MeV}$. The solid line is obtained with $\mu_{\rm P} = 1.793$, the dashed line is with $\mu_{\rm P} = 1.71$, the dotted line is with $\mu_{\rm P} = 2.01$. The data are taken from NIKHEF [16].

If the electron and the outgoing proton are described as plane waves, the reduced cross-section

$$\rho_m(p_m) = \frac{1}{PE_{\rm P}\sigma_{\rm eP}}\frac{{\rm d}^3\sigma}{{\rm d}E_f\,{\rm d}\Omega_f\,{\rm d}\Omega_{\rm P}}, \tag{13}$$

is the probability, that the proton, bound in a given shell, is met inside the nucleus with momentum $-\mathbf{p}_m$ (the missing momentum is defined by $\mathbf{p}_m = -(\mathbf{P}-\mathbf{q})$). The (off-shell) electron-proton cross-section $\sigma_{\rm eP}$ denotes the form "cc1" by de Forest [19].

In our analysis, we account for the Coulomb distortion of the electron. The calculation is performed for parallel kinematics only, where the outgoing proton momentum $\mathbf{P}$ is along the momentum transfer $\mathbf{q}$. The SF for a given shell is determined for various values of $\mu_{\rm P}$ by scaling the theoretical calculations for $\rho_m(p_m)$ to fit the experimental data [16,17] by minimizing χ^2. All curves are calculated by changing the anomalous magnetic moment $\mu_{\rm P}$ value in ref. [11] for proton.

In fig. 1, we show the reduced cross-section as a function of the missing momentum p_m corresponding to knocking out the proton from the $1d_{3/2}$ orbit in ^{40}Ca. The ini-

tial electron energy is $E_{\rm i} = 375\,{\rm MeV}$, the energy transfer $\omega = 100\,{\rm MeV}$, and the momentum transfer $q = 430\,{\rm MeV/c}$ at $p_m = 0\,{\rm MeV/c}$. The solid line is calculated with $\mu_{\rm P} = 1.793$, which is the experimental value of the free proton, the dashed and the dotted lines are the results with $\mu_{\rm P} = 1.71$ and $\mu_{\rm P} = 2.01$ (for the bound proton), respectively. The experimental data are from NIKHEF [16]. The deviation of the dotted line from the solid line is 6% at the peak on the left side, where the momentum transfer is around $q = 560\,{\rm MeV/c}$, and it is around 3% on the right side, where $q = 320\,{\rm MeV/c}$; the effect of the form factor due to the swollen proton is relatively larger in the high momentum transfer region (high negative missing momentum region) rather than on the small momentum transfer region (high positive missing momentum region). Figure 2 shows the calculation for the $2s_{1/2}$ orbit in ^{40}Ca for the same kinematics as in fig. 1. The deviation between the solid line and the dotted line is 4% at the first peak position and it also decreases in the higher positive missing momentum region. Over the whole region of the missing momentum under our calculations, the effect of the anomalous magnetic moment increases with higher negative missing momentum, which means, the bound nucleon has large momentum. Note that SF values used for these curves are $S_{d_{3/2}} = 0.8$ and $S_{2s_{1/2}} = 0.75$ in ref. [1] for figs. 1 and 2, respectively.

Figure 3 shows the behavior of the SF *versus* the anomalous magnetic moment for each state. While this SF drops rapidly up to $\mu_{\rm P} = 1.793$, it decreases slowly on higher magnetic moment. Since the SF values are correlated with the $\mu_{\rm P}$ they are somewhat sensitive to $\mu_{\rm P}$. In table 1, we compare the SF values extracted from our analysis with those obtained by other groups. The SF values in ref. [3] were obtained with a relativistic single-particle model for a bound state like ours. The factors in refs. [5, 16] were calculated with the RPA and the nonrelativistic analysis, respectively. As shown, the SF values are sensitive to the wave functions used, but also depend on the form factor effect more or less.

We also consider ^{208}Pb as a next target nucleus. Figures 4 and 5 show a comparison of the reduced cross-sections from $3s_{1/2}$ and $2d_{3/2}$ orbits with different anomalous magnetic moments. The initial electron energy is $E_{\rm i} = 412.3\,{\rm MeV}$ and the kinetic energy of the outgoing proton is $T_{\rm P} = 100\,{\rm MeV}$. In these cases, the momentum transfer is $q = 445\,{\rm MeV/c}$ at $p_m = 0\,{\rm MeV/c}$. Again the solid lines are the result for $\mu_{\rm P} = 1.793$, the dashed lines for $\mu_{\rm P} = 1.71$, and the dotted lines for $\mu_{\rm P} = 2.01$. The differences between the solid lines and the dotted lines are 8% at the first peak for $3s_{1/2}$ and 10% at the left peak ($q = 510\,{\rm MeV/c}$) and 5% at the right first peak ($q = 350\,{\rm MeV/c}$) for $2d_{3/2}$. As in the case of ^{40}Ca, the effect increases with large q. These curves are multiplied with $S_{3s_{1/2}} = 0.71$ for $3s_{1/2}$ and $S_{2d_{3/2}} = 0.8$ for $2d_{3/2}$. Again, in fig. 6, we show the dependence of the SF values on $\mu_{\rm P}$. The decreasing rate of the SF for ^{208}Pb is similar to the ^{40}Ca for each orbit while the slopes have different values. We also compare the SF values to each other in table 2.

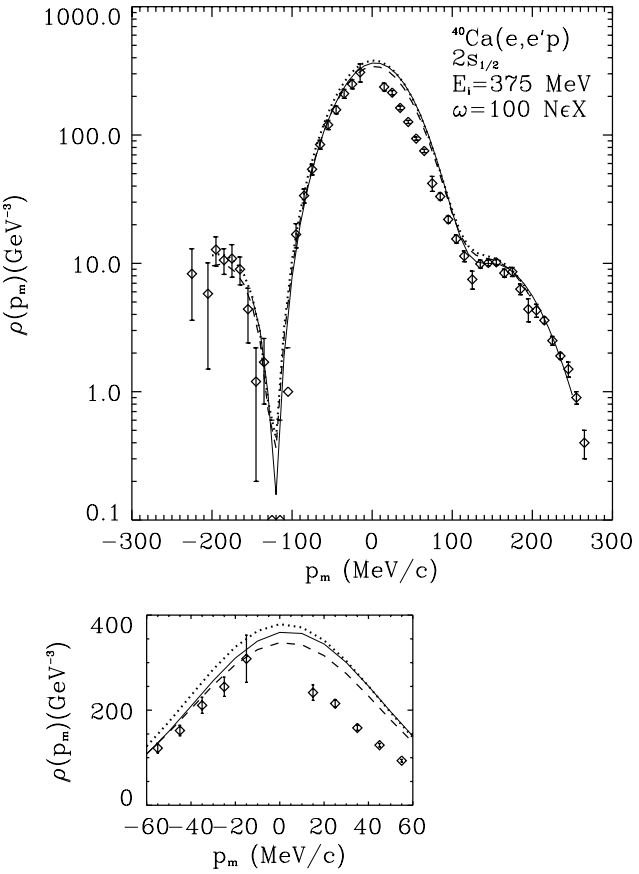

Fig. 2. The same as fig. 1 but for the $2s_{1/2}$ orbit.

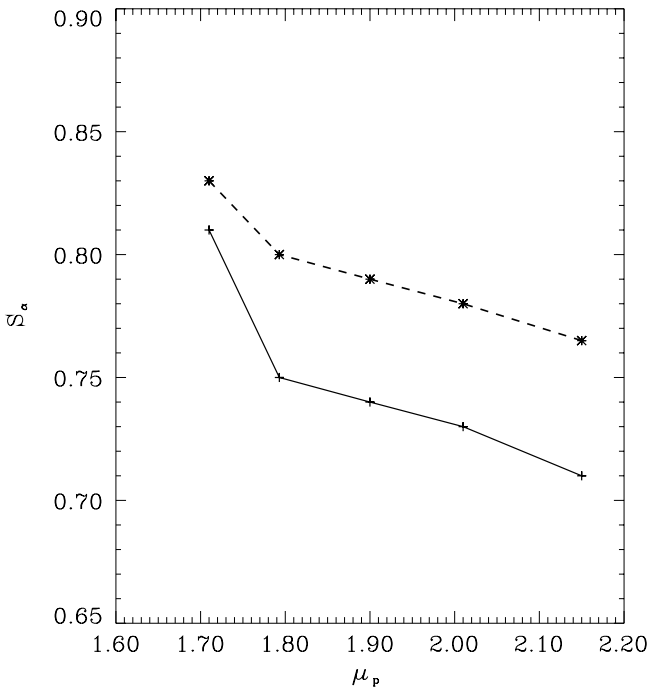

Fig. 3. The SF values with respect to anomalous magnetic moments for ^{40}Ca. The solid line is for $2s_{1/2}$ and the dashed line for $1d_{3/2}$.

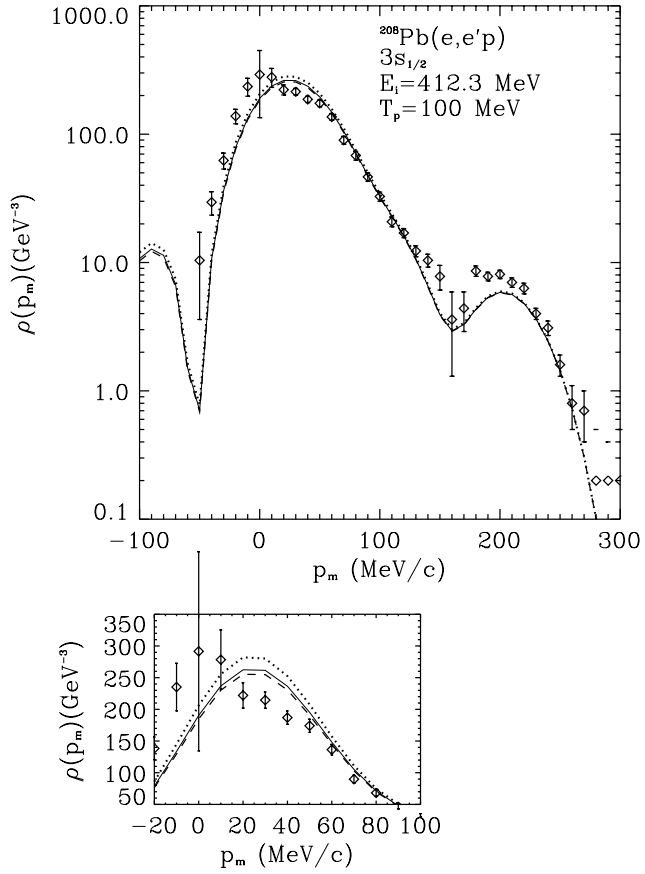

Fig. 4. The reduced cross-sections for ^{208}Pb from the $3s_{1/2}$ orbit with parallel kinematics. The kinematics are $E_{\rm i}$ = 412.3 MeV, and energy transfer $T_{\rm P}$ = 100 MeV. The solid line is used $\mu_{\rm P}$ = 1.793, the dashed line is $\mu_{\rm P}$ = 1.71, the dotted line is $\mu_{\rm P}$ = 2.01, the data are from NIKHEF [17].

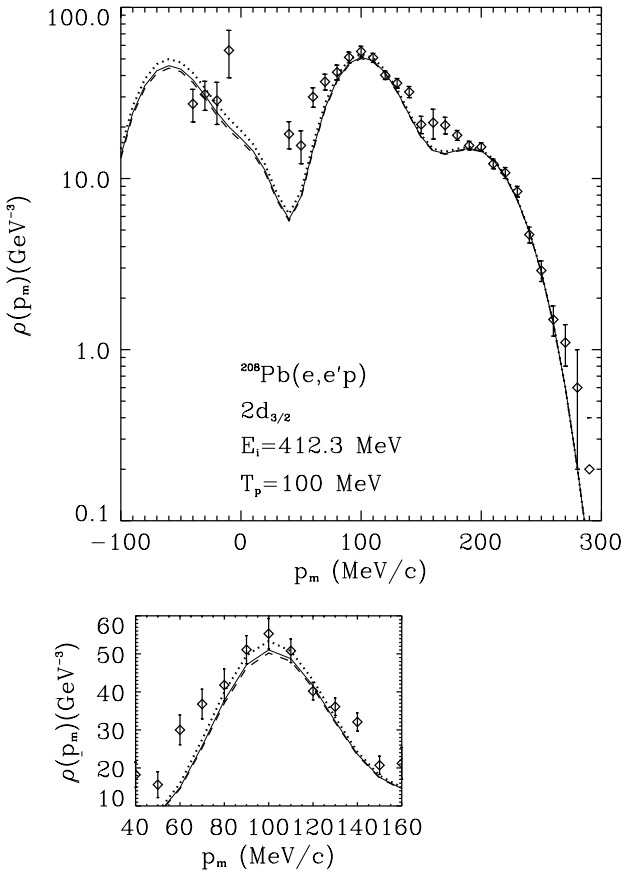

Fig. 5. The same as fig. 4 but for the $2d_{3/2}$ orbit.

In fig. 7, we show the curve in the χ^2 minimizing procedure per experimental data with respect to the $\mu_{\rm P}$ values. The solid and the dotted lines are for $2s_{1/2}$ and for $1d_{3/2}$ of ^{40}Ca and the dashed and the dash-dotted lines are for $3s_{1/2}$ and $2d_{3/2}$ of ^{208}Pb, respectively. The three curves for $2s_{1/2}$ and $d_{3/2}$ of ^{40}Ca and $2d_{3/2}$ of ^{208}Pb have clearly the minimum position in χ^2 as a function of $\mu_{\rm P}$. And then, the minimum positions are placed between $\mu_{\rm P}$ values 1.0 and 2.0. But, in case of $3s_{1/2}$ of ^{208}Pb, there is no minimum position.

4 Conclusion

The purpose of this work in the (e, e′p) process is to study the effect of the form factor containing an anomalous magnetic moment, which is obtained with effective masses of mesons and nucleons in the framework of the cloudy bag model. The SF decreases slowly for higher anomalous magnetic moment while the χ^2 per data values increase rapidly on higher magnetic moment. The experimental data are sensitive to the anomalous magnetic moment $\mu_{\rm P}$ because of the existence of the minimum position in χ^2. The q-dependence of our ansatz for the swollen nucleon plays a

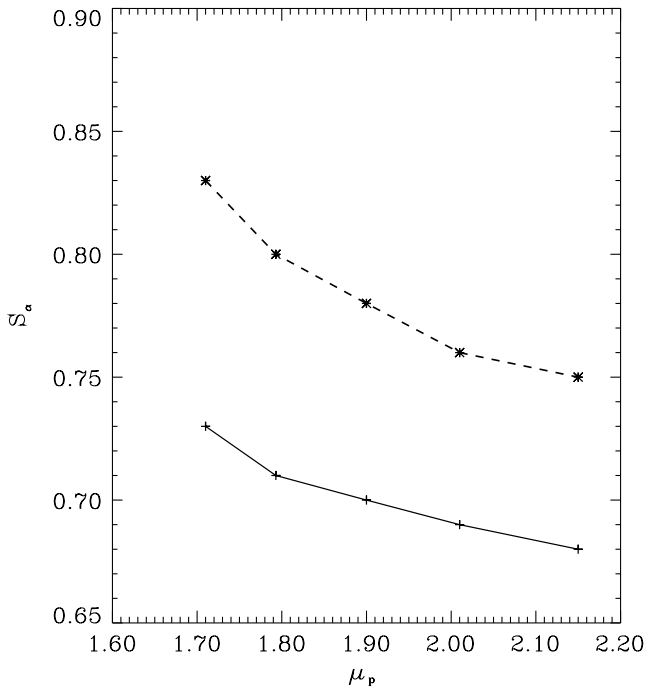

Fig. 6. The SF values with respect to anomalous magnetic moments for ^{208}Pb. The solid line is for $3s_{1/2}$ and the dashed line for $2d_{3/2}$.

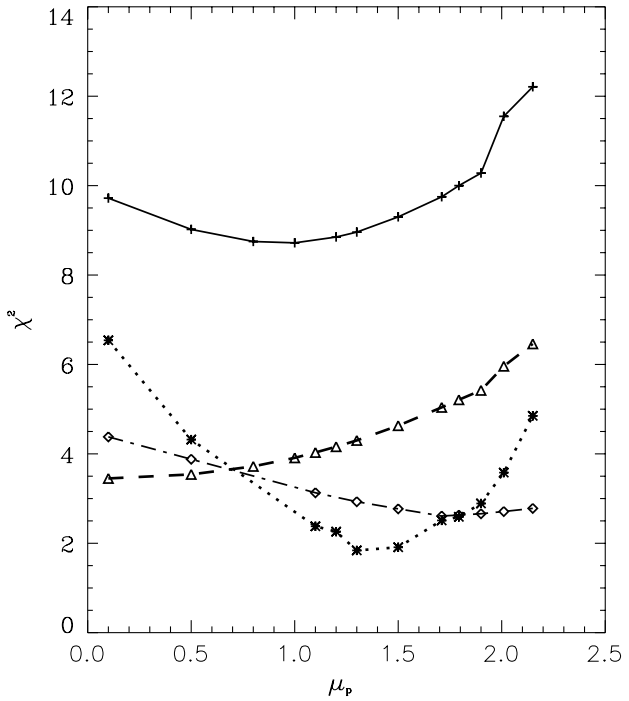

Fig. 7. The χ^2 values with respect to anomalous magnetic moments for ^{40}Ca and ^{208}Pb. The solid and the dotted lines are for $2s_{1/2}$ and for $1d_{3/2}$ of ^{40}Ca and the dashed and dash-dotted lines are for $3s_{1/2}$ and $2d_{3/2}$ of ^{208}Pb, respectively.

Table 1. The comparison with other values of spectroscopic factors for ^{40}Ca.

Orbit	This work	ref. [1]	ref. [3]	ref. [16]	ref. [5]
$1d_{3/2}$	0.78	0.8	0.76	0.65	0.60
$2s_{1/2}$	0.73	0.75	0.51	0.51	0.48

Table 2. The comparison with other values of spectroscopic factors for ^{208}Pb.

Orbit	This work	ref. [1]	ref. [3]	ref. [17]	ref. [5]
$3s_{1/2}$	0.69	0.71	0.70	0.40	0.51
$2d_{3/2}$	0.76	0.8	0.73	0.46	0.54

larger role in the larger nucleus under the condition of the particular data under investigation in this paper.

However, there still remain problems before final conclusion can be drawn. One of them comes from the errors on the experimental data which are not small enough to distinguish between the different calculations. Namely, the deviation between all curves are smaller than the error bars in the figures. Other ambiguities stem from the off-shell properties of the bounded nucleon as commented on the prelude. Therefore, without significantly more accurate experimental data and significantly better control on the theoretical ambiguities in these calculations, it will be impossible to see the effects of the medium-modified nucleon form factors in the (e, e′p) reaction. Since the off-shell properties and the correlations of the nucleons are believed to have some relationship with each other, one needs to continue studying such relations in this reaction. It might be possible to furnish the effect of the swollen nucleon in the nuclear medium if much improved theoretical interpretations were applied to this work.

This work was supported by the Korean Ministry of Education under Grant No. BSRI-98-2425 and the Korean Science and Engineering Foundation.

References

1. Yanhe Jin, D.S. Onley, L.E. Wright, Phys. Rev. C **45**, 1311 (1992).
2. K.S. Kim, L.E. Wright, Phys. Rev. C **56**, 302 (1997).
3. J.M. Udias, P. Sarriguren, E. Moya de Guerra, E. Garrido, J.A. Caballero, Phys. Rev. C **48**, 2731 (1993).
4. V. Van der Sluys, J. Ryckebush, M. Waroquier, Phys. Rev. C **54**, 1322 (1996).
5. V. Van der Sluys, J. Ryckebush, M. Waroquier, Phys. Rev. C **55**, 1982 (1997).
6. B.D. Serot, Phys. Lett. B **86**, 146 (1979).
7. C.J. Horowitz, B.D. Serot, Nucl. Phys. A **368**, 503 (1981).
8. A. Bouyssy, J.-F. Mathiot, Nguyen Van Giai, S. Marcos, Phys. Rev. C **36**, 380 (1987).
9. M.K. Cheoun, A. Bobyk, F. Simkovic, A. Faessler, G. Teneva, Nucl. Phys. A **561**, 74 (1993); Nucl. Phys. A **587**, 301 (1995).
10. K.S. Kim, M.K. Cheon, Il-Tong Cheon, Y. Cheng, J. Korean Phys. Soc. **35**, 399 (1999).
11. Il-Tong Cheon, Moon Taeg Jeong, J. Phys. Soc. Jpn., **61**, 2726 (1992); Moon Taeg Jeong, Il-Tong Cheon, Phys. Rev. D **43**, 3725 (1991).
12. W.M. Alberico, P. Czerski, M. Ericson, A. Molinari, Nucl. Phys. A **462**, 269 (1987).
13. G.E. Brown, C.B. Dover, P.B. Siegel, W. Weise, Phys. Rev. Lett. **60**, 2723 (1988).
14. J.J. Kelly, Phys. Rev. C **59**, 3256 (1999); *Effects of spinor distortion and density-dependent form factors upon quasifree* ^{16}O(**e**, e′**p**), nucl-th/9905024, 1999.
15. S. Hama, B.C. Clark, E.D. Cooper, H.S. Sherif, R.L. Mercer, Phys. Rev. C **41**, 2737 (1990).
16. G.J. Kramer, Ph.D. dissertation, University of Amsterdam, 1990; G.J. Kramer *et al.*, Phys. Lett. B **227**, 199 (1989).
17. Edwin Quint, Ph.D. dissertation, University of Amsterdam, 1988.
18. Z.E. Meziani *et al.*, Phys. Rev. Lett. **52**, 2130 (1984).
19. T. de Forest Jr., Nucl. Phys. A **392**, 232 (1983).